Solid State Sciences 12 (2010) 1168–1172

Contents lists available at ScienceDirect

Solid State Sciences

journal homepage: www.elsevier.com/locate/ssscie

Determining Seebeck coefficient of heavily doped La:$SrTiO_3$ from density functional calculations

Rui-zhi Zhang*, Chun-lei Wang, Ji-chao Li, Wen-bin Su, Jia-liang Zhang, Ming-lei Zhao, Jian Liu, Yan-fei Zhang, Liang-mo Mei

School of Physics, State Key Laboratory of Crystal Materials, Shandong University, Jinan 250100, People's Republic of China

ARTICLE INFO

Article history:
Received 6 June 2009
Received in revised form
31 March 2010
Accepted 31 March 2010
Available online 8 April 2010

Keywords:
Thermoelectric
Boltzmann transport theory
Density of states
Density functional theory

ABSTRACT

A novel approach was developed to calculate temperature-dependent Seebeck coefficient of heavily doped systems. The electronic density of states (DOS) and Fermi energy were determined and then, using these two parameters, the Seebeck coefficient was calculated by using Boltzmann transport theory. This approach is applied to heavily La-doped $SrTiO_3$. The calculated Seebeck coefficient agrees well with the experimental data. By analyzing the results, it was shown that Seebeck coefficient is greatly affected by the asymmetry of DOS with respect to Fermi energy.

1. Introduction

Thermoelectric (TE) materials are of great interest because these materials can be used to convert heat to electrical power [1]. The efficiency of the conversion depends on the dimensionless figure of merit, $ZT = S^2\sigma T/\kappa$, where S, σ, κ and T are the Seebeck coefficient, electrical conductivity, thermal conductivity and absolute temperature, respectively. In general, larger ZT value provides more efficiency of heat-to-electric conversion, and the practical applications of TE materials require $ZT \geq 1$. Therefore much effort was spent on the searching for TE materials with large ZT value. For this purpose, theoretical predictions of the TE transport coefficients are very helpful. Currently, there are mainly two theoretical methods for TE properties predictions. One is empirical formula fitting [2,3], in which the empirical formulas are used with some fitting parameters, such as the electronic effective mass and the carrier concentration [2,3]. However, this method cannot predict TE properties of new materials whose experimental data is too rare to construct the fitting formulas. Alternatively, the other method based upon density functional theory (DFT) calculations can be used to solve this problem [4,5].

In the DFT-based methods, no fitting parameter from the experiment is needed. The band structure is *ab initio* calculated by DFT, then the electronic group velocity is derived from the band structure, and transport coefficients can be determined by using the Boltzmann transport equation. This method was quite successful for the transport coefficients calculations of lightly doped systems by using the 'rigid band model', in which doping is introduced by adjusting the Fermi energy and the band structure is assumed to be the same for both doped and undoped systems [4,5]. This assumption is reliable only when the system is lightly doped. While for heavily doped systems, the 'rigid band model' is no longer reliable, because the dopant concentration is so high that its influence on the band structure of the host material is not negligible. An alternative approach is discarding 'rigid band model' and calculating the band structure of a *doped* supercell directly, while this approach introduces the 'band crossing' problem [6]. The 'band crossing' problem is caused by the dopants breaking the lattice symmetry and making the degenerate bands split. It makes the determination of the electronic group velocity and the transport coefficients inaccurate. Therefore a reliable method for transport coefficients calculation of heavily doped system should be established.

In this paper, we develop a new method to calculate Seebeck coefficient of heavily doped systems. In order to eliminate the electron group velocity inaccuracy caused by band crossing, the transport coefficient is calculated by using the electronic density of

* Corresponding author. Tel.: +86 0531 88377035 8323; fax: +86 531 88377031.
E-mail address: rzzhang@mail.sdu.edu.cn (R.-z. Zhang).

1293-2558/$ – see front matter © 2010 Elsevier Masson SAS. All rights reserved.
doi:10.1016/j.solidstatesciences.2010.03.021

states (DOS) instead of the group velocity. This method is applied to 12.5%, 6.2% and 3.7% La-doped $SrTiO_3$(La:STO). La:STO has been reported as a promising TE oxide material [7,8], and the experimental data of the single crystal are available [2,3], which provide a good reference to evaluate the accuracy of our calculation.

2. Method: multi-band model

From the Boltzmann transport equation and the relaxation time approximation, the Seebeck coefficient of *a single band* can be expressed as [9]:

$$S_i = \frac{\int g_i(E)E\left(E-E_f\right)\frac{\partial f_0}{\partial E}dE}{eT\int g_i(E)E\frac{\partial f_0}{\partial E}dE} \quad (1)$$

where $g(E)$, E_f, τ_e, f_0, e, and T are the electronic DOS, Fermi energy, relaxation time, Fermi distribution, charge of an electron and absolute temperature, respectively. τ_e is treated as a constant in this equation, which was a reliable approximation in transport coefficients calculation [4,5,10]. Therefore when the DOS $g_i(E)$ and the Fermi energy E_f are obtained, the temperature-dependent Seebeck coefficient of a single band can be determined.

As the Seebeck coefficient of each single band can be determined by using Eq. (1), we now can turn to the multi-band case, i.e. there are several bands near the Fermi surface which contribute to electrical transport. This is more general, because usually there are both light electrons (electrons with low effective mass) and heavy electrons in the conduction band. The *total* Seebeck coefficient can be expressed as

$$S = \frac{\sum_i \sigma_i S_i}{\sum_i \sigma_i} \quad (2)$$

where S, σ_i, and S_i are the total Seebeck coefficient, electrical conductivity of a single band and Seebeck coefficient of a single band, and the sum runs over all bands. For a parabolic band, the electrical conductivity of *a single band* is

$$\sigma_i = \frac{2e^2}{3m^*}\int g_i(E)\tau_e E\frac{\partial f_0}{\partial E}dE \quad (3)$$

where $g_i(E)$, τ_e, f_0, e, m^* and T are the electronic DOS, relaxation time, Fermi distribution, charge of an electron, electronic effective mass and absolute temperature, respectively. σ_i cannot be calculated from DFT calculations because τ_e is unknown. Actually, τ_e is usually obtained from the experimental data in previous theoretical work [4,5,10]. Hence in this work the electrical conductivity will not be calculated from Eq. (3) straightforwardly and further work is needed to calculate τ_e from DFT calculations [11–13]. In this paper, the total Seebeck coefficient can be calculated without knowing the value of τ_e, because τ_e can be treated as a constant and it is in both numerator and denominator in Eq. (2). Therefore the only unknown parameter is the effective mass m^*. For a parabolic band, $g_i(E)$ can be expressed as a function of m^*

$$g_i(E) = V\frac{4\pi}{h^3}(2m^*)^{3/2}E^{1/2} \quad (4)$$

where V and h are supercell volume and Planck's constant, respectively. Using Eqs. (3) and (4), we have

$$\sigma_i \propto \int g_i(E)^{1/3}E^{4/3}\frac{\partial f_0}{\partial E}dE \quad (5)$$

From Eqs. (1)–(5), the temperature-dependent Seebeck coefficient can be determined by using $g_i(E)$ and E_f. The calculation details of determining these two parameters by DFT calculations will be described in Section 4.

3. Computation details

The DFT calculations were performed using plane wave-pseudopotential method as implemented in Quantum-ESPRESSO package [14]. Perdew–Burke–Ernzerhof [15] generalized gradient approximation (GGA) was used for the exchange–correlation functional, and ultrasoft pseudopotentials [16] were used for all atoms. Sr *4s 4p 4d 5s* Ti *3s 3p 4s 3d* O *2s 2p* and La *5s 5p 5d 6s 6p* orbitals were treated as valence orbitals. A plane wave basis with kinetic energy cutoff of 30 Ry is used to ensure the convergence in all the calculations.

Firstly, an STO primitive unit cell (UC) was optimized to determine the lattice constants by using the damp method [17]. An $8 \times 8 \times 8$ Monkhorst–Pack [18] (MP) k-points was used, which is well tested to give convergent results. The optimization stops when the stress along each direction is less than 0.5 kbar. The optimized lattice constant is 3.928 Å, which agrees well with experimental results 3.905 Å [19]. Then using this lattice constant value, three types of supercells are constructed with the following extensions of the primitive unit cell vectors: $2 \times 2 \times 2$ for 8-UC supercell,$2\sqrt{2} \times 2\sqrt{2} \times 2\sqrt{2}$ for 16-UC supercell and $3 \times 3 \times 3$ for 27-UC supercell. The 16-UC supercell was created by using Evarestov's method [20]. Then doping was introduced by substituting a La atom for a Sr atom in each supercell. Therefore the 8-UC, 16-UC, and 27-UC supercells correspond to 12.5%, 6.2%, and 3.7% doping concentrations, respectively. Then geometry optimization of the doped supercells is performed and the MP k-points are: $4 \times 4 \times 4$, $3 \times 3 \times 3$, and $2 \times 2 \times 2$ for 8-UC, 16-UC, and 27-UC supercells, respectively. The optimization stops when all components of force on each atom are less than 10^{-3} a.u. The optimized supercells are used to calculate electronic DOS, which will be used for the Seebeck coefficient calculations.

4. Results and discussion

4.1. DOS calculation

According to Eqs. (1) and (5), the accuracy of transport coefficients calculation mostly relies on the accuracy of DOS, especially near the band edge. The k-points sampling is very important for the accuracy of DOS. Therefore a convergence of k-point testing is done and we find that a k-grid of $20 \times 20 \times 20$, $8 \times 8 \times 8$ and $6 \times 6 \times 6$ are sufficient for 8-UC, 16-UC and 27-UC supercells, respectively. Such dense k-grids are needed mainly because of the partial filling of the energy bands near the Fermi surface, as La:STO is a metallic system.

Then the methods of DOS calculations are compared. In general, there are two methods: the smearing method [21,22] and the tetrahedron method [6]. The smearing method is widely used for DOS calculations of both insulate and metallic system as it gives smooth DOS shape by using relatively few k-points [21,22]. In this method, a Gaussian boarding linewidth W is needed. Smaller value of W can give more precise DOS, while a much denser k-grid is needed to get convergence [23]. In the limit of $W \rightarrow 0$ the 'absolute' DOS can be obtained. As a certain value of W is always used for including the effect of temperature on DFT band structure calculations, the DOS calculated by this method is not exact, especially near the band edge due to the Gaussian boarding in smearing. Alternatively, tetrahedron method [6] is more accurate in the calculation of DOS. The DOS calculated from both methods are shown in Fig. 1(a). The Gaussian boarding W for smearing

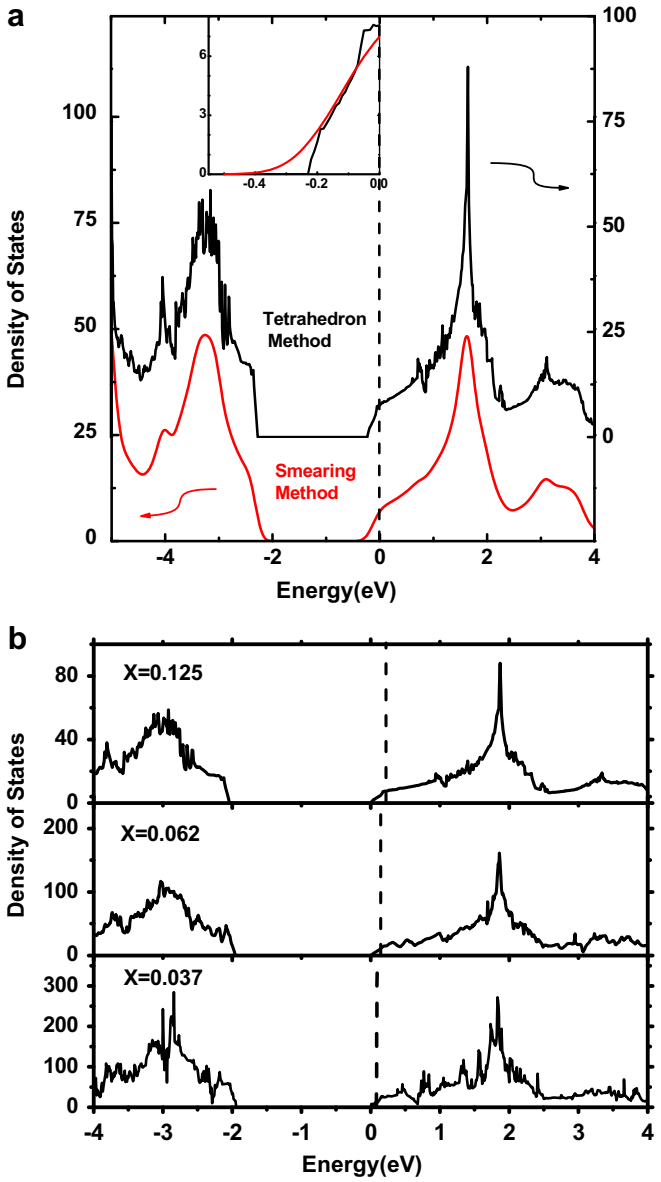

Fig. 1. (a) DOS of $La_{0.125}$ $Sr_{0.875}$ TiO_3. Upper (black) and lower (red) parts correspond to DOS form tetrahedron method and smearing method, respectively. Dotted line is Fermi level. The inset shows DOS near the conduction band edge. (b)DOS of La_x Sr_{1-x} TiO_3 systems ($x = 0.125$, 0.062 and 0.037). Conduction band edge was set as zero, and Fermi levels were denoted by dotted lines. (For interpretation of the references to colour in this figure legend, the reader is referred to the web version of this article.)

method is 0.01 Ry, and a k-grid of $20 \times 20 \times 20$ is needed to give convergent result. From Fig. 1(a), it can be seen that the DOS shapes from the two methods are similar, and both agree with the DOS obtained by inverse-photoemission spectroscopy (IPES) measurement [24], indicating that our k-points sampling is sufficient. The main difference of the two DOS lies near the band edge, as shown in the inset of Fig. 1(a). To further illustrate which method is more accurate, the 'exact' band gap is calculated from the band structure, i.e. $E \sim k$ dispersion along high symmetry lines in Brillouin zone. The band gap from band structure is exact because the band edge always locates in high symmetry lines. The band gap from the band structure is 2.0 eV, which is the same as 2.0 eV from tetrahedron method but larger than 1.6 eV from the smearing method. This suggests that the tetrahedron method is more accurate for calculating the DOS.

Fig. 1(b) shows the DOS of 8-UC, 16-UC and 27-UC supercells, corresponding to 12.5%, 6.2% and 3.7% La doping. The conduction band minimum was set to zero, and Fermi energy was denoted by a dashed line. It can be seen that the Fermi energy lies in the conduction band in all these doping systems, indicating their metallic behavior. Furthermore, Fermi energy shifts to higher energy as doping concentration increases, that is, 0.09 eV for 3.7%, 0.15 eV for 6.2% and 0.22 eV for 12.5% La doping. The Fermi energy given here is at 0 K, as DFT only calculates the ground-state properties. The Fermi energy at a certain temperature will be determined in the next section.

In addition, the density states effective mass m_d^* are calculated from the DOS by using Eq. (4). The m_d^* is an important parameter for thermoelectric properties, as many researchers in thermoelectric filed use m_d^* for the calculation of Seebeck coefficient. By fitting the DOS according to Eq. (4), m_d^*/m_0 is determined to be 5.12 for 3.7%, 4.85 for 6.2% and 4.74 for 12.5% La-doped STO, respectively, where m_0 is the mass of a free electron. Our results are in good agreement with experimental value 4.2 [25] and other theoretical calculations [26,27].

4.2. Fermi energy determination

In general, there are two methods in the determination of temperature-dependent Fermi energy. One is the correction for metal (CFM), which is convenient and reliable when $E_f^0 >> k_B T$

$$E_f = E_f^0\left[1 - \frac{\pi^2}{12}\left(\frac{k_B T}{E_f^0}\right)^2\right] \tag{6}$$

where E_f, E_f^0, T and k_B are the Fermi energy at a certain temperature, Fermi energy at 0 K, absolute temperature and Boltzmann constant, respectively. After E_f^0 was determined from DFT calculations, the temperature-dependent Fermi energy can be obtained by using Eq. (6). The other method, the Fermi integral (FI), is more general. FI can be expressed as:

$$n = \int g(E) f_0 dE \tag{7}$$

where n, $g(E)$ and f_0 are the carrier concentration, DOS and Fermi–Dirac distribution, respectively. The Fermi energy is involved in f_0. In La:STO, n is equal to the dopant concentration, because all the La dopants are ionized even at low temperature [2]. Moreover, the carriers concentration is nearly a constant for different temperatures, because the band gap of STO is very large (about 3.2 eV [28]) and intrinsic carriers can be neglected. As Fermi energy E_f^0 and carrier concentration n are known, the temperature-dependent Fermi energy is determined by using these two methods, respectively.

Fig. 2 shows the temperature-dependent Fermi energy for 12.5%, 6.2% and 3.7% La:STO, respectively. It can be seen that for 12.5% La:STO, the Fermi energy calculated from CFM and FI is nearly the same, which means at such a high doping level $E_f^0 >> k_B T$, i.e. the Fermi energy is far from the conduction band edge. On the other hand, in 6.2% and 3.7% La:STO, there are large discrepancies in CFM and FI results. This is because the doping concentration is too low and the Fermi energy lies close to conduction band edge, which causes CFM to lose its validity. Therefore, in the Seebeck coefficient calculations, FI is used to determine the temperature-dependent Fermi energy.

4.3. Seebeck coefficient calculation and analysis

As DOS and Fermi energy are both determined from DFT calculations, Seebeck coefficient can be calculated by using Eqs.

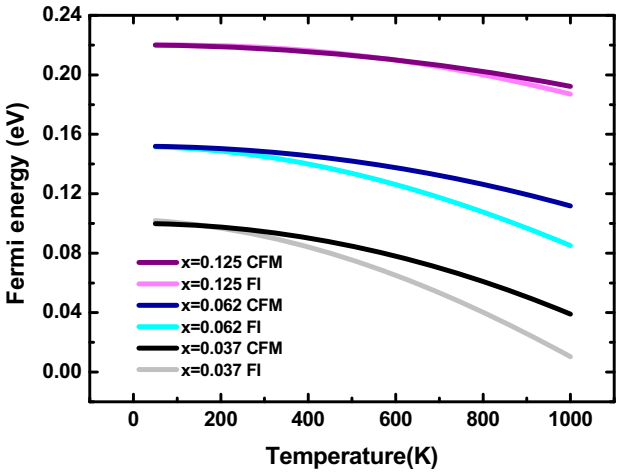

Fig. 2. Temperature-dependent Fermi energy of $La_xSr_{1-x}TiO_3$ systems($x = 0.125$, 0.062 and 0.037) calculated by using the Fermi integrals (FI) and the correction for metal (CFM), respectively.

(1)–(5). Fig. 3 shows the temperature-dependent Seebeck coefficient of three La-doped supercells. Experimental data are also plotted for comparison. The experimental data below 300 K are of 5% La:STO [2], and the experimental data above 300 K are of 6.8×10^{20} cm^{-3} carrier concentration La:STO [3]. The La:STO in both experiments are single crystal. So the comparison of theoretical and experimental results is quite reasonable because in DFT calculations the supercells represent infinite single crystal. From Fig. 3, it can be seen that the theoretical results of 3.7% La:STO agree well with the experimental data. Below 300 K, the theoretical Seebeck coefficient is larger than experimental data, this is because the theoretical doping level (3.7%) is smaller than experimental doping level (5%) and Seebeck coefficient decreases as doping level increases [3]. Above 300 K, the theoretical and experimental systems have nearly the same carrier concentration (about 6.8×10^{20} cm^{-3}), so our method underestimates the Seebeck coefficient. This is because in our approach the relaxation time is assumed to be a constant, based on the consideration that the electrons contributing to transport are in a narrow energy range due to the delta-function like Fermi broadening, and relaxation time is nearly the same for the electrons in such a narrow energy range. This assumption is reasonable at low temperature, while at high temperature it is no longer reliable as Fermi broadening

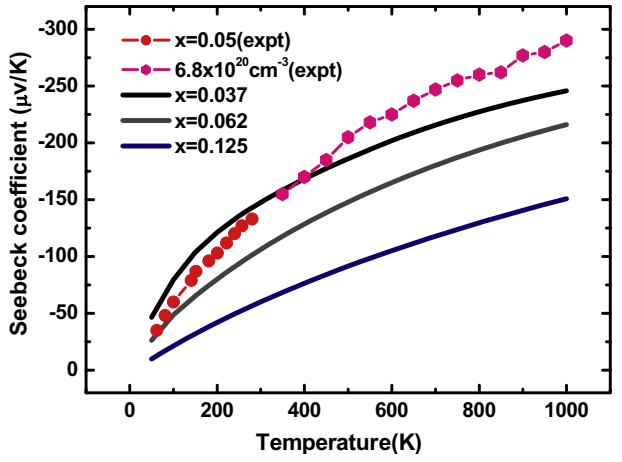

Fig. 3. Temperature-dependent Seebeck coefficient of $La_xSr_{1-x}TiO_3$ systems ($x = 0.125$, 0.062 and 0.037). The experimental data are also shown for comparison.

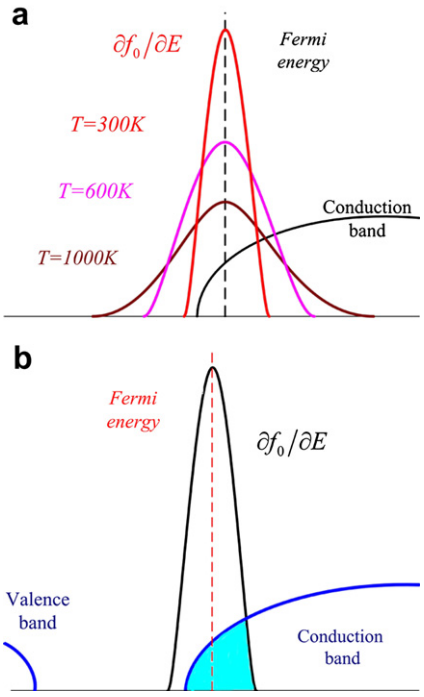

Fig. 4. (a) schematic diagram of temperature-dependent Fermi boardening. (b) Schematic diagram of the DOS asymmetry with respect to Fermi energy.

enlarges, as shown in Fig. 4(a). Therefore further work is needed to calculate the temperature-dependent relaxation time.

Furthermore, there are two trends of the theoretical Seebeck coefficient in Fig. 3: first, the Seebeck coefficient increases with decreasing doping level; and second, the Seebeck coefficient increases with increasing temperature. These can be understood by analyzing the asymmetry of DOS with respect to Fermi energy, which is shown by shaded areas in Fig. 4(b). From Eq. (1), Seebeck coefficient depends on the asymmetry of DOS, i.e. difference in DOS below and above the Fermi energy [29]. Larger asymmetry, which is caused by the lower Fermi energy, provides larger Seebeck coefficient. As shown in Figs. 1(b) and 2, when doping level decreases or temperature increases, the Fermi energy will be lowered, which increases the Seebeck coefficient by enlarging the asymmetry of DOS with respect to the Fermi energy.

5. Conclusions

A novel approach is present to calculate the temperature-dependent Seebeck coefficient of heavily doped systems. Other than using the group velocity, in this approach the DOS and Fermi energy obtained from DFT calculations are used. This approach is applied to La:STO. In the DOS calculations, the tetrahedron method is more accurate than the smearing method, especially near the band edge. And in the Fermi energy determination, FI is more reliable than CFM for these heavily doped systems. The theoretical Seebeck coefficient is compared with the experimental data and well agreement is found. The theoretical Seebeck coefficient is analyzed and it is shown that the Seebeck coefficient greatly depends on the asymmetry of DOS with respect to the Fermi energy.

Acknowledgements

The work is financially supported by National Basic Research Program of China of 2007CB607504 and Natural Science Fund of China under grant No. 50572052 and 50902086.

References

[1] G. Mahan, B. Sales, J. Sharp, Phys. Today 50 (1997) 42.
[2] T. Okuda, K. Nakanishi, S. Miyasaka, Y. Tokura, Phys. Rev. B 63 (2001) 113104.
[3] S. Ohta, T. Nomura, H. Ohta, K. Koumoto, J. Appl. Phys. 97 (2005) 034106.
[4] T.J. Scheidemantel, C. Ambrosch-Draxl, T. Thonhauser, J.V. Badding, J.O. Sofo, Phys. Rev. B 68 (2003) 125210.
[5] L. Chaput, P. Pecheur, J. Tobola, H. Scherrer, Phys. Rev. B 72 (085126) (2005).
[6] P.E. Blochl, O. Jepsen, O.K. Andersen, Phys. Rev. B 49 (1994) 16223.
[7] S. Ohta, T. Nomura, H. Ohta, M. Hirano, H. Hosono, K. Koumoto, Appl. Phys. Lett. 87 (2005) 092108.
[8] H. Ohta, S. Kim, Y. Mune, T. Mizoguchi, K. Nomura, S. Ohta, T. Nomura, Y. Nakanishi, Y. Ikuhara, M. Hirano, H. Hosono, K. Koumoto, Nat. Mater. 6 (2007) 129.
[9] G.S. Nolas, J. Sharp, H.J. Goldsmid, Thermoelectrics: Basic Principles and New Materials Development. Springer, Berlin, 2001.
[10] T. Thonhauser, T.J. Scheidemantel, J.O. Sofo, J.V. Badding, G.D. Mahan, Phys. Rev. B 68 (2003) 085201.
[11] B.-L. Huang, M. Kaviany, Phys. Rev. B 77 (2008) 125209.
[12] J. Sjakste, N. Vast, V. Tyuterev, Phys. Rev. Lett. 99 (2007) 236405.
[13] F. Bertazzi, M. Moresco, E. Bellotti1, J. Appl. Phys. 106 (063718) (2009).
[14] S. Baroni, A. Dal Corso, S. de Gironcoli, P. Giannozzi, et al. http://www.pwscf.org.
[15] J.P. Perdew, K. Burke, M. Ernzerhof, Phys. Rev. Lett. 77 (1996) 3865.
[16] D. Vanderbilt, Phys. Rev. B 41 (1990) 7892.
[17] M. Parrinello, A. Rahman, Phys. Rev. Lett. 45 (1980) 1196.
[18] H.J. Monkhorst, J.D. Pack, Phys. Rev. B 13 (1976) 5188.
[19] T. Mitsui, S. Normura (Eds.), Numerical Data and Functional Relations in Science and Technology – Crystal and Solid State Physics, Landolt-Bornstein, New Series, Group III, vol. 16, Pt. A, Springer, Berlin, 1982.
[20] R.A. Evarestov, S. Piskunov, E.A. Kotomin, G. Borstel, Phys. Rev. B 67 (2003) 064101.
[21] M. Methfessel, A.T. Paxton, Phys. Rev. B 40 (1989) 3616.
[22] N. Marzari, D. Vanderbilt, A. De Vita, M.C. Payne, Phys. Rev. Lett. 82 (1999) 3296.
[23] A.D. Corso, Lecture Notes in Chemistry. Springer, Berlin, 1996.
[24] T. Higuchi, T. Yasuhisa, T. Hattori, S. Yamaguchi, S. Shin, T. Tsukamoto, Jpn. J. Appl. Phys. 43 (2004) 7623.
[25] R. Moss, A. Gnudi, K.H. Hardtl, J. Appl. Phys. 78 (1995) 5042.
[26] W. Wunderlich, H. Ohta, K. Koumoto, Physica B Condens. Matter. 404 (2009) 2202.
[27] W. Wunderlich, K. Koumoto, Int. J. Mater. Res. 97 (2006) 657.
[28] K. van Benthem, C. Elsasser, R.H. French, J. Appl. Phys. 90 (2001) 6156.
[29] G.D. Mahan, J.O. Sofo, Proc. Natl. Acad. Sci. 93 (1996) 7436.